Tectonophysics, 197 (1991) 295–308
Elsevier Science Publishers B V , Amsterdam

Constraints on rift propagation history at the Cobb Offset, Juan de Fuca Ridge, from numerical modeling of tectonic fabric

Tom Shoberg [a], Seth Stein [a] and Jill Karsten [b]

[a] *Department of Geological Sciences, Northwestern University, Evanston, IL 60208, USA*
[b] *Hawaii Institute of Geophysics, University of Hawaii, Honolulu, HI 96822, USA*

(Received April 5, 1990; revised version accepted June 26, 1990)

ABSTRACT

Shoberg, T., Stein, S. and Karsten, J., 1991. Constraints on rift propagation history at the Cobb Offset, Juan de Fuca Ridge, from numerical modeling of tectonic fabric. In: A.F. Gangi (Editor), World Rift Systems. *Tectonophysics*, 197: 295–308.

Rift propagation has been proposed as the mechanism for the reorganization of the Juan de Fuca Ridge during the Cenozoic. In particular, magnetic anomalies in the Cobb Offset region of this ridge have been interpreted in terms of a complex "dueling propagator" history, in which rift propagation has occurred alternately in opposing directions on adjacent ridge segments. Although the overall propagation history has been inferred from the magnetic data, these data are limited in their resolution for the detailed history by the length of time during which magnetic polarity remains constant. We thus examine whether more detailed resolution within polarity chrons can be obtained using seafloor tectonic fabric from acoustic imagery. By modeling lineations as isochrons, synthetic fabric can be generated for a given rift propagation history and the fit of the model to the data can be compared numerically. For the Cobb, we used a propagation history model with a given timing and direction of propagation, and generated synthetic fabric for different propagation rates. The fabric is best fit for propagation rates between 400 and 900 mm/yr. Slower (< 300 mm/yr) propagation rates yield significantly poorer fits, whereas faster (> 900 mm/yr) propagation rates yield slightly poorer fits. The fabric results are thus in accord with the interpretation, based on magnetics alone, that the rates of rift propagation significantly exceeded the spreading rates. An interesting feature of the model is that the complex tectonic fabric is reasonably well fit on this scale (~ 1 km) by simple rift propagation models which do not invoke shear zone behavior and thus deviate from rigid plate tectonics.

Introduction

The geometry of oceanic spreading centers often evolves by rift propagation (Hey, 1977; Hey et al., 1980), a process in which one ridge segment lengthens at the expense of an adjacent segment, which is preempted and ceases spreading (Fig. 1). The locus of relative motion between the two plates shifts from the dying rift to the growing one, such that the rift tips are joined by a transform fault which migrates with time, transferring lithosphere from one plate to the other. Structural discontinuities, known as pseudofaults, bound seafloor formed at the growing ridge during propagation. Seafloor isochrons between the propagating and failed rifts, which were formed prior to rift propagation, are reoriented when they are transferred between plates. The angle through which the isochrons are reoriented depends on the ratio of spreading rate to propagation velocity (Searle and Hey, 1983; Acton et al., 1988). Rift propagation thus gives rise to characteristic magnetic anomalies and seafloor structures oblique to both spreading center and transform fault trends. In this simple propagation model, spreading instantly ceases on the dying ridge and begins on the growing ridge. Thus the oblique structures resulting from the lineation reorientation form as a consequence of rigid plate tectonics because, at any time, motion occurs only at discrete plate boundaries. Rift propagation has been used to describe the tectonic evolution of a variety of past and present midocean ridge systems, including the Cocos–Nazca spreading center (Hey and Vogt, 1977; Searle and Hey, 1983; Hey et al., 1986; Miller and Hey, 1986; Acton et al., 1988), the East

0040-1951/91/$03.50

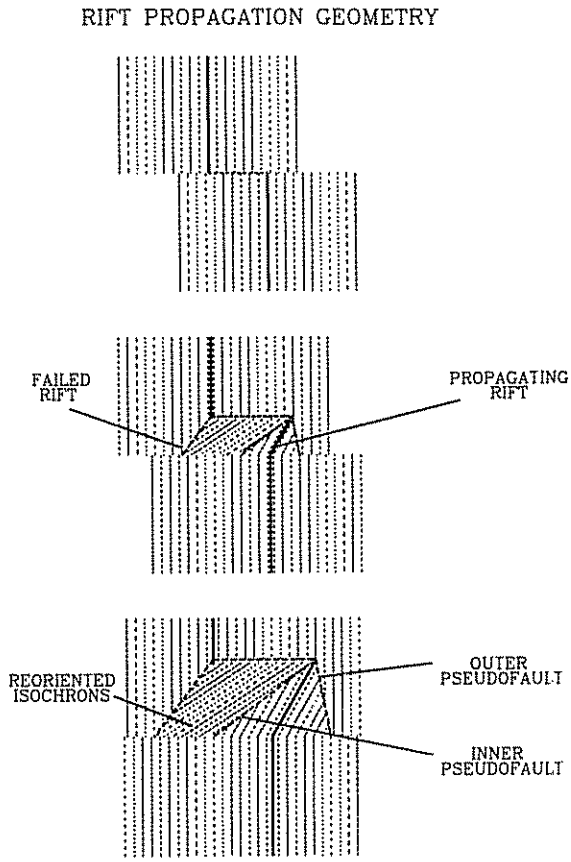

Fig. 1. Schematic of rift propagation geometry showing ridge segments (heavy lines), isochrons, pseudofaults and reoriented isochrons.

Pacific Rise (Mammerickx, 1984; Engeln and Stein, 1984; Hey et al., 1985; Anderson-Fontana et al., 1986; McKenzie, 1986; Naar and Hey, 1986; Francheteau et al., 1987; Engeln et al., 1988; Macdonald et al., 1988; Mammerickx et al., 1988; Lonsdale, 1989), and the Gulf of Aden and Afar region (Courtillot et al., 1980; Vink, 1982; Acton et al., 1990).

In these studies, the overall propagation history has been successfully inferred from magnetic data. These data, however, are limited in their resolution for the detailed history by the length of time during which magnetic polarity remains constant. This limitation poses difficulties for studies of small-scale propagating rift systems, perhaps including overlapping spreading centers where all the seafloor between the growing and dying ridges formed during the current magnetic polarity chron (within 730,000 yr). It seems natural to attempt to derive more detailed resolution within polarity chrons by assuming that much of the tectonic fabric in young oceanic lithosphere recorded by imaging systems such as Gloria, Seabeam, or Seamarc, represents structures formed at the ridge axis. Seafloor features having trends that satisfy this assumption can thus be modeled as isochrons, and compared to the synthetic fabric predicted by a model of the spreading history. This technique has been applied with some success to regions including the Galapagos propagator (McKenzie, 1986; Acton et al., 1988) and the Easter microplate (Engeln et al., 1988), and can provide valuable insight into seafloor formed by a complex spreading history.

Our goal is to explore the constraints on rift propagation history that can be derived from tectonic fabric modeling. We focus on the Juan de Fuca Ridge in the northeast Pacific, where marine magnetic data have been interpreted as indicating a complex propagation history (Hey, 1977; Hey and Wilson, 1982; Johnson et al., 1983; Wilson et al., 1984; Stoddard, 1987; Wilson, 1988; Atwater, 1989). A complex propagation history has been inferred for the Cobb Offset (Fig. 2) along this ridge. Johnson et al. (1983) demonstrate that an unusual magnetic anomaly pattern can be interpreted as the result of two "dueling propagators". In this model, propagation events repeatedly alternated between two ridge segments which grew at the expense of the other. We attempt to use the tectonic fabric to verify and, if possible, refine this model.

The Cobb Offset

At the Juan de Fuca Ridge, the Pacific and Juan de Fuca plates are spreading apart at a full rate of about 60 mm/yr (Raff and Mason, 1961; Vine and Wilson, 1965; Vine, 1966; Riddihough, 1977; Nishimura et al., 1984). The ridge geometry has evolved throughout most of the Tertiary by rift propagation (Hey, 1977; Hey et al., 1980; Carlson, 1981; Hey and Wilson, 1982; Johnson et al., 1983; Wilson et al., 1984; Karsten et al., 1986; Stoddard, 1987; Wilson, 1988). A portion of the ridge of particular interest (Fig. 2) is the Cobb Offset, at about 47.5°N, 129°W, which separates

the Northern Symmetrical Ridge (NSR) segment from the Endeavour segment. Currently, the two ridge segments overlap for about 30 km, and are separated by about 30 km in the overlap region. For convenience, we use the term "overlap" without implying that the overlapping ridge segments spread simultaneously.

A striking feature of the magnetic anomaly data (Fig. 2b) is that the area formed during the Brunhes normal chron is composed of two wedge-shaped regions, one southward pointing on the Endeavour segment and one northward pointing on the NSR segment. Hey and Wilson (1982) identified the wedge boundaries as pseudofaults indicating northward rift propagation. Johnson et al. (1983), however, noted additional features which make it possible to refine the rift propagation history. An anomalously wide zone of reversely magnetized crust (asterisk in Fig. 2b) adjacent to the Olduvai anomaly on the Pacific side led them to infer that propagation occurred prior to the episode indicated by the tapered Brunhes anomaly. Second, Johnson et al. used locations where unaltered basaltic glass was recovered by dredging and where freshly extruded basalts were photographed to define the present trace of the northernmost active NSR segment. Based on these observations, they inferred that the locus of active spreading on the NSR trends northwesterly from the center of the region of Brunhes normal crust. A subsequent Seabeam study (Karsten et al., 1986) also supports this interpretation. This model has

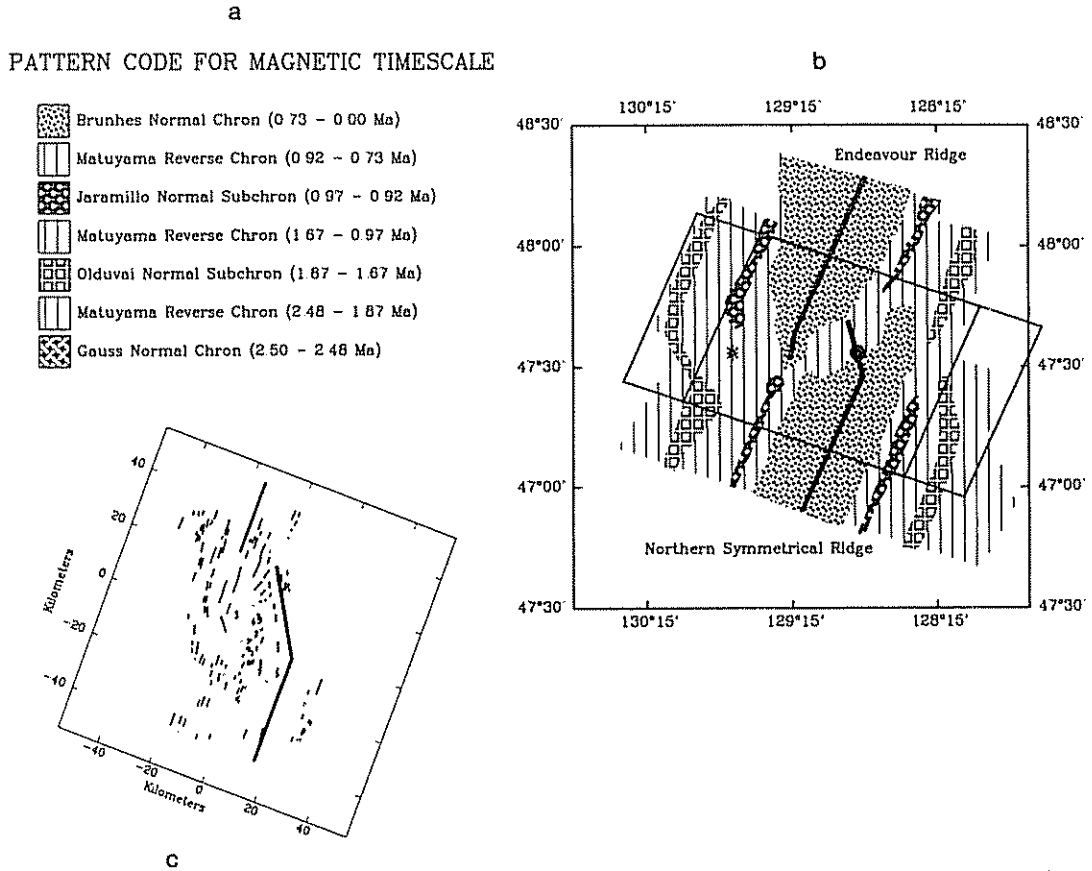

Fig. 2. Data used to constrain the rift propagation models. (a) The patterns associated with the magnetic data of Johnson et al. (1983). These are slightly different than that used in the subsequent synthetic models where it is possible to subdivide the Matuyama reversed chron. (b) The magnetic data of Johnson et al. (1983). The inset large and small boxes represent the area of coverage of the subsequent magnetic and fabric synthetics. The asterisk shows the location of the wide zone of reversed crust noticed by Johnson et al., and the dot represents the location of the Surveyor volcano. (c) The fabric data, interpreted from Davis et al. (1987), with the thick solid line representing the current modeled spreading center configuration.

TABLE 1

Parameters used in rift propagation simulation

Propagation event	Starting age (Ma)	Propagation azimuth (°CW-N)	Distance of propagation (km)	Spreading rate-JDF (mm/yr)	Spreading rate-PAC (mm/yr)	Spreading azimuth (°CW-N)
	2.50	0	0.0	29.0	29.0	270
1	1.70	150	36.0	29.0	29.0	270
2	1.35	0	28.0	29.0	29.0	270
		330	8.0			
3	0.99	150	8.0	29.0	29.0	270
4	0.72	0	13.0	29.0	30.0	270
		330	12.0			
5	0.40	180	28.0	29.0	30.0	270
		150	8.0			
6	0.1–0.05	330	33.0	29.0	30.0	270

The propagation distances were taken directly from Johnson et al. (1983). The starting time, spreading rates and azimuths and the propagation azimuth were slightly modified from the Johnson et al. model to yield the best fit to the magnetics.

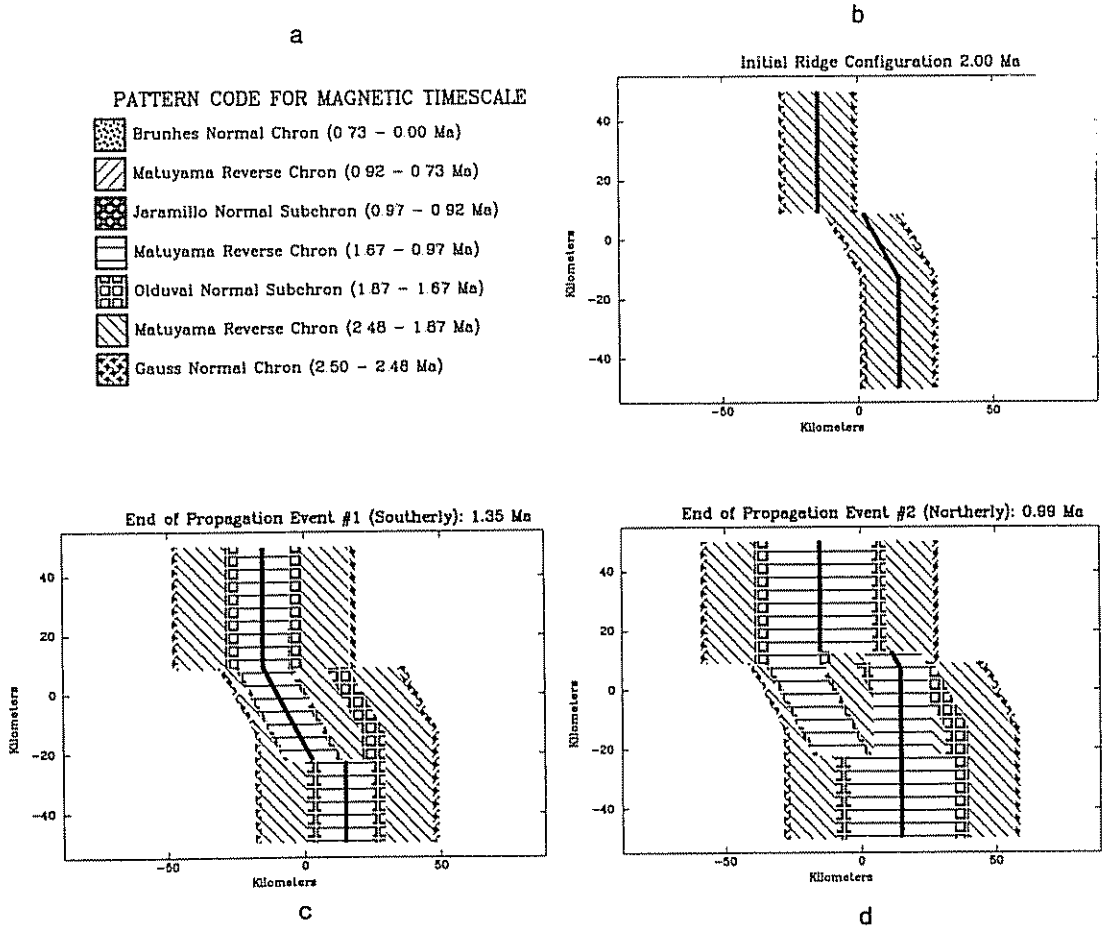

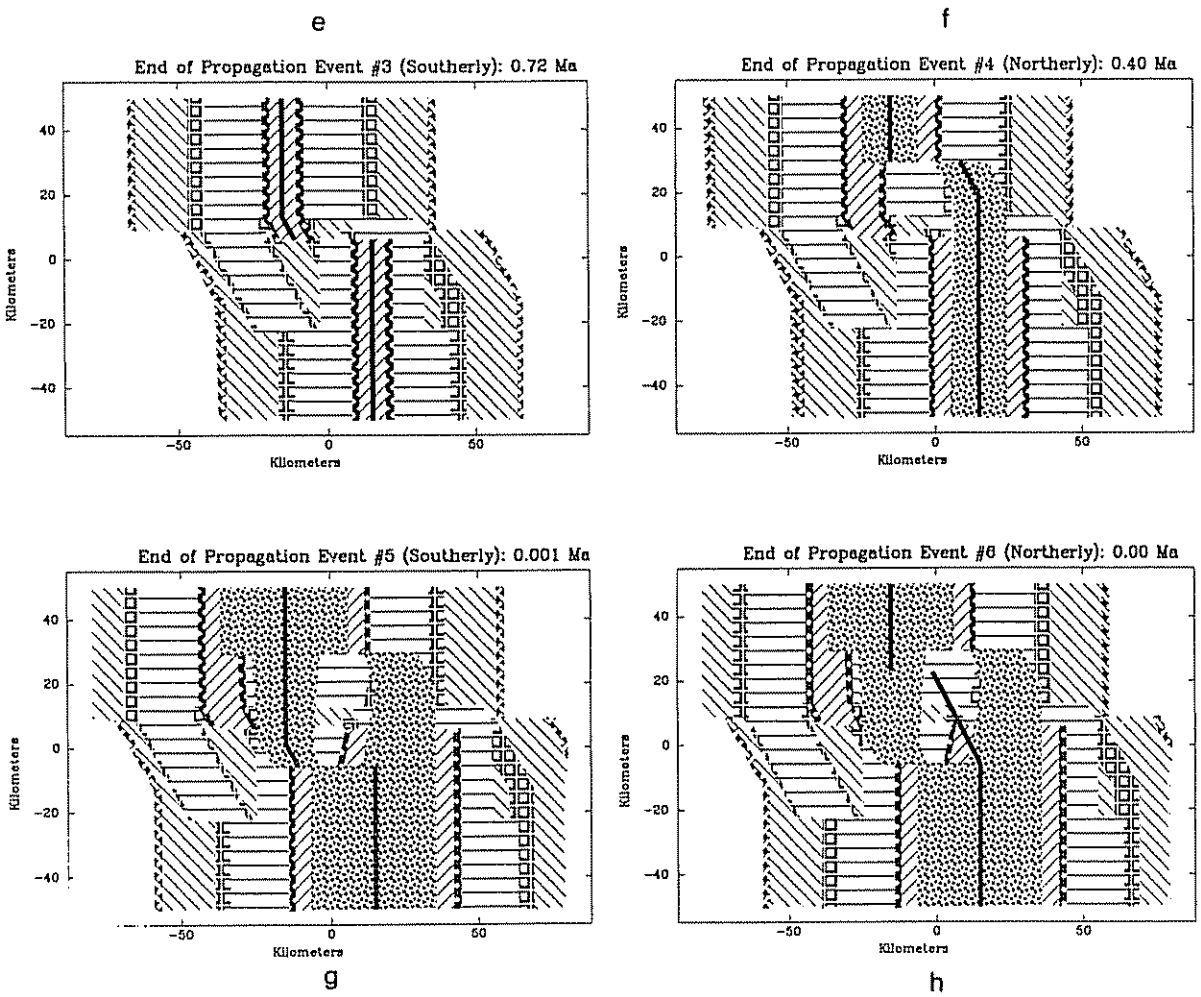

Fig. 3. Dueling propagator history modified from Johnson et al. (1983). (a) Magnetic timescale pattern used in this and subsequent figures. (b–h) The sequence of propagation events modeled by Johnson et al. for an instantaneous propagator. Each panel shows the magnetic isochron pattern at the end of its respective event (Table 1).

the unusual feature that the propagating NSR tip does not bisect the wedge of Brunhes age crust, and has no observable magnetic signature, presumably because it started spreading only very recently.

Johnson et al. (1983) proposed two models to explain these observations. The models require both northward propagation by the NSR segment and southward propagation by the Endeavour segment. In one, propagation has been predominantly northward, and both overlapping ridges spread simultaneously and asymmetrically, such that no spreading occurs on the overlapping flanks. However, in their preferred model northward and southward, propagation events alternate. In this model, only one of the overlapping ridges is active, and spreads symmetrically. This "dueling propagation" behavior is unusual, as most propagation events occur in a single direction (e.g. Wilson et al., 1984).

Figure 3 illustrates the "dueling propagation" model. A curved ridge configuration at 2 Ma is postulated to accommodate the curvature of the Olduvai anomaly on the Juan de Fuca side of the NSR segment and on the Pacific side of the Endeavour segment. During a sequence of propagation events (Table 1), either the southern segment propagated northward or the northern segment propagated southward. For each event, the timing, azimuth of propagation, and distance

covered during the event are specified. Some propagation events were divided into two subevents, during which the azimuth of propagation changed. The magnetic anomalies strongly constrain the propagation distance and provide a looser constraint on the time of propagation events, because an event only needs to terminate before the next magnetic reversal. Note that the wide region of reversely magnetized crust adjacent to the Olduvai anomaly on the Pacific side results from event 2 (Fig. 3d) and that the recent NSR configuration forms in event 6 (Fig. 3h).

Whether the overlapping portions of both segments are currently spreading is uncertain. Johnson et al. assume that spreading has recently ceased on the overlapping portion of the Endeavour segment and has shifted to the new location of the NSR segment. They note, however, that their models are insensitive to spreading on both ridges in the overlap zone at present.

An interesting feature of the Johnson et al. model for the fine (~ 10 km) scale features of the Cobb Offset is that the rift propagation in alternating directions was assumed to occur rapidly with respect to the spreading rates. In contrast, the Wilson et al. (1984) regional model described larger-scale features with only northward propagation at rates comparable to the spreading rates. We thus seek to test how well the propagation rate for the evolution of the Cobb Offset can be estimated from the available data.

Data

Because our primary data are the magnetic anomalies from Johnson et al., our models are naturally a refinement on their work. Additionally, we use seafloor fabric lineations. Fabric can constrain tectonic models only by assuming something about its origin. The simplest assumption is that the lineations are isochrons, so that their trends can be predicted for a given tectonic history. If this is the case, tectonic fabric data are more sensitive than magnetic data to the details of the propagation within a polarity chron (Acton et al., 1988). Hence by incorporating the lineation data, we hoped to obtain more detailed resolution than provided by the magnetic data alone.

For this purpose, we used tectonic fabric taken from a Seamarc acoustic imagery map of the North Central Juan De Fuca Ridge compiled by Davis et al. (1987). We digitized 157 lineations which could not unambiguously be associated with some extraneous volcanism, such as at a seamount, and compiled the fabric dataset shown in Fig. 2c. The lineations range from 2 to 15 km in length and are less than 0.5 km in width.

An important feature of the data is the large number of lineations within the overlap region of the Cobb Offset. These lineations are oblique to the trends of the boundaries between polarity chrons, except where chrons are truncated by pseudofaults (Fig. 2b). The most useful constraint on the propagation models comes from the lineations oriented approximately NE–SW, which appear to have been reoriented by the propagation.

The present positions of the ridge segments are taken from the bathymetry (Karsten et al., 1986). They show that Surveyor Volcano (Fig. 2b) has been split into halves ~ 3 km apart, implying (for a 60 mm/yr full spreading rate) that this section of the NSR has been active for about the last 50,000 yrs. Unfortunately, their data also indicates the presence of three large seamounts and several minor ones in the area, which slightly complicate the fabric and magnetic anomaly analysis. The lineations are not numerous compared to other ridges, presumably due to the high sedimentation rate in this area (Karsten et al., 1986).

Model

We began by examining the fit of a variety of models for the evolution of the Cobb Offset to the magnetic data. The models covered from 2.6 Ma to the present, which includes two normal polarity chrons, one reverse polarity chron and two normal polarity subchrons. As expected, the most successful model geometry, spreading rates, and propagation sequence (Table 1) are essentially those of Johnson et al. At 2.5 Ma, the two ridge segments trend N22°E and are offset by 30 km. We assumed symmetric spreading with a 58 mm/yr full rate from 2.5–0.72 Ma, and a slight asymmetry (3.5%) with the Pacific plate faster during the Brunhes. This is well within the error limits associ-

ated with the Euler vectors determined by Nishimura et al. (1984).

To model synthetic isochrons from the propagating rifts, we followed the Johnson et al. propagation history. We assumed the simplest possible propagator kinematics, in whic ..ding is instantaneously transferred from the dying to the propagating ridge, such that rigid plate tectonics applies, and neither a microplate nor a shear zone forms. Because we used a time step of 1000 years and generated synthetic isochrons every 50,000 years, events of duration of less than a few thousand years would not be visible in the models.

After adopting the propagation history listed in Table 1, we tested the effect of rift propagation rates between 100 and 1000 mm/yr. Because the age of the onset of propagation, and the distance covered during each event were kept fixed, the propagation rate determined the duration of propagation. Once the required distance was covered, spreading was assumed to continue smoothly with no propagation. Each rate was assumed to apply for all propagation events, except for the 100 mm/yr case in which the final event required a 330 mm/yr rate to yield the present ridge configuration. Propagation rates less than 100 mm/yr were excluded by the magnetic data because insufficient crust would be formed. For comparison to Johnson et al.'s results, we generated a model with an infinite propagation rate for all events except event 5, which generated the tapered Brunhes anomalies. For the other events, the magnetic data alone provide only a lower bound on the rate.

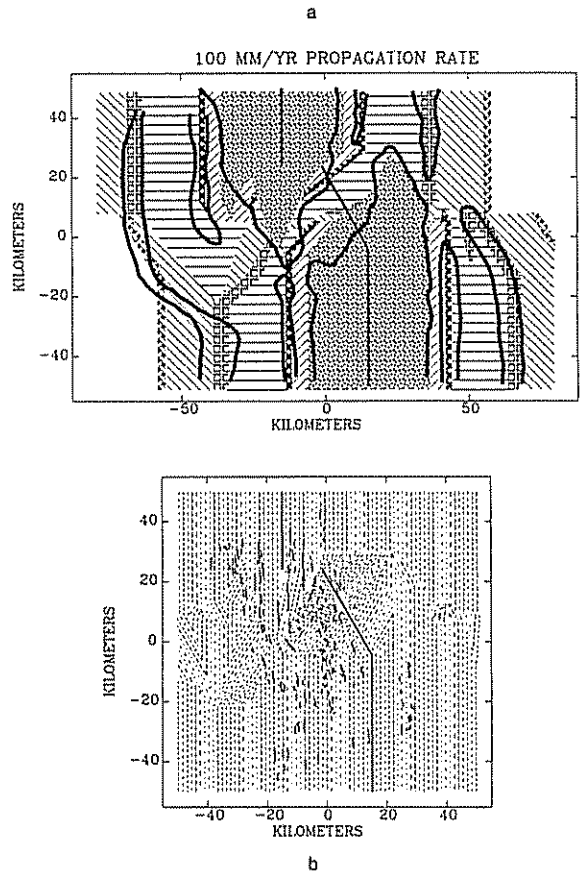

Fig. 4. Comparison of the observed data to the synthetics for the 100 mm/yr model; (a) magnetics. (b) fabric. (Patterns are the same as in Fig. 3.) Both plots show considerable discrepancy between the synthetics and the observations in the overlap region. The predicted fabric elements (dashed lines) generally trend clockwise relative to the data (short thick lines) within the overlap area.

Results

Figures 4, 5 and 6 show the model predictions and the data, magnetic and fabric, for three propagation rates. For convenience, the figures are centered at 47.54°N, 129.07°W and rotated such that N22°E is toward the top of the page. All of the models fit the bathymetric constraints equally well.

For the magnetics, the thick solid lines (Fig. 2b) enclose the observed normal polarity chrons and subchrons. The synthetic timescale pattern is the same as in Fig. 3. As expected, the data are generally well fit. There are, however, several difficulties. The predicted thin normal polarity (Jaramillo) zones within the offset region are not shown by the data, but this situation is complicated by the Surveyor Volcano (Fig. 2b). The predicted Brunhes anomaly for the southern Endeavour segment is narrower than observed, perhaps indicating two stages of propagation during event 5. Johnson et al. interpret the Olduvai anomaly west of the Endeavour segment as continuous but offset with that west of the NSR. Neither their model nor ours yield this continuity. The data used in their model, however, are sparse in this area. The SW Olduvai anomaly is predicted to be narrower than observed, a situation possibly complicated by a seamount in the area.

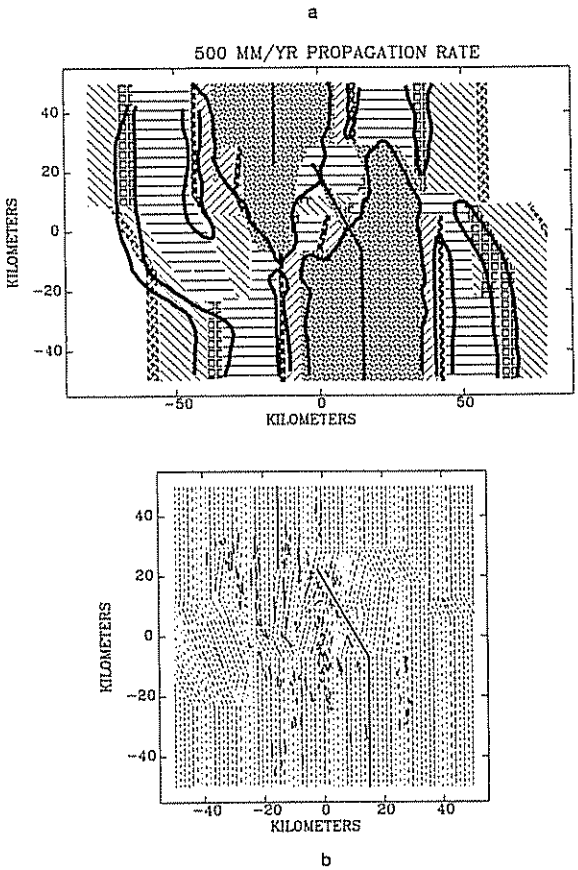

Fig 5 Comparison of the observed data to the synthetics for the 500 mm/yr model; (a) magnetics. (b) fabric (Patterns are the same as in Fig 3.) Most of the lineations in the overlap region are well fit by the predicted fabric This constitutes the best fit

Comparison of the figures for the different propagation rates shows the resolution obtainable from the magnetic data alone. The 100 mm/yr model (Fig. 4) has the most difficulties. It predicts a region of Olduvai age crust extending SW from the southern tip of the Brunhes age crust on the Endeavour segment, whereas the data show no such normal polarity region. Similarly, on the western sides of both segments, the predicted Brunhes age crust protrudes beyond the observed boundary. In contrast, the 1000 mm/yr model (Fig. 6) predicts a region of reversely magnetized crust within the observed Brunhes region on the western flank of the NSR and Brunhes crust outside the tips of the observed Brunhes wedges. On balance, the model shown with an intermediate propagation rate, 500 mm/yr (Fig. 5), yields a better fit to the magnetic data than those with 100 or 1000 mm/yr rates.

Figures 4, 5 and 6 also show the predicted and observed fabric overlays for these three propagation rates. The fabric north and south of the overlap region is essentially ridge-parallel and is well fit by all the models, none of which include propagation in these areas. This agreement provides some support for the assumption that lineations can be treated as isochrons. The most interesting difference between the models is in their ability to predict the approximately NE–SW lineations in the overlap region. These trends are fit reasonably well by the 500 mm/yr model, less well by the 1000 mm/yr model and significantly worse by the 100 mm/yr model. This effect occurs because these trends have been reoriented from ridge-parallel by an angle inversely proportional

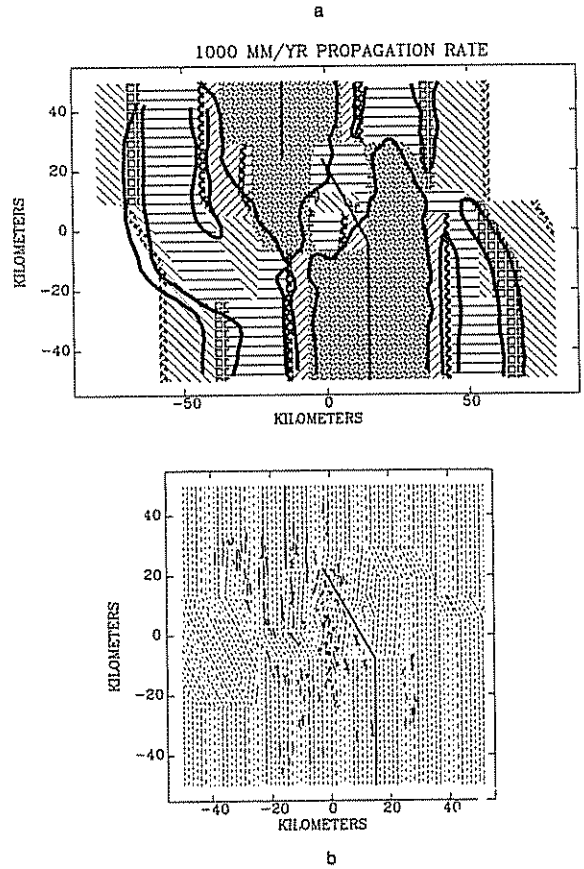

Fig 6 Comparison of the observed data to the synthetics for the 1000 mm/yr model; (a) magnetics. (b) fabric (Patterns are the same ins Fig 3.) The synthetic fabric significantly misfit the data in the overlap zone

to the propagation rate, since the spreading rate is fixed. Thus for the 100 mm/yr propagation rate model, the predicted fabric generally trends clockwise from those observed, indicating that this rate is too slow. In contrast, for the 1000 mm/yr propagation rate model, the predicted fabric generally trends counter-clockwise from those observed, indicating too fast a rate. Note that the distance between isochrons is reduced after reorientation and the pseudofaults appear only as boundaries between lineation sets.

There are, however, some systematic misfits to all models. The data show lineations along and subparallel to the most recent trend of the NSR. Because the models assume that this segment formed recently, as required by the absence of Brunhes polarity crust, these trends are not well predicted especially east of the NSR. A longer period of spreading on the most recent trend of the NSR would yield the observed lineations, but this crust would be normally magnetized. It is unclear whether this difficulty reflects the limitations of the data, the model, or the complexity of the early evolution of a propagating ridge. A less serious, but interesting, effect is that the predicted trends of the isochrons are systematically biased clockwise to those observed, perhaps suggesting adjustments to the initial ridge geometry. This

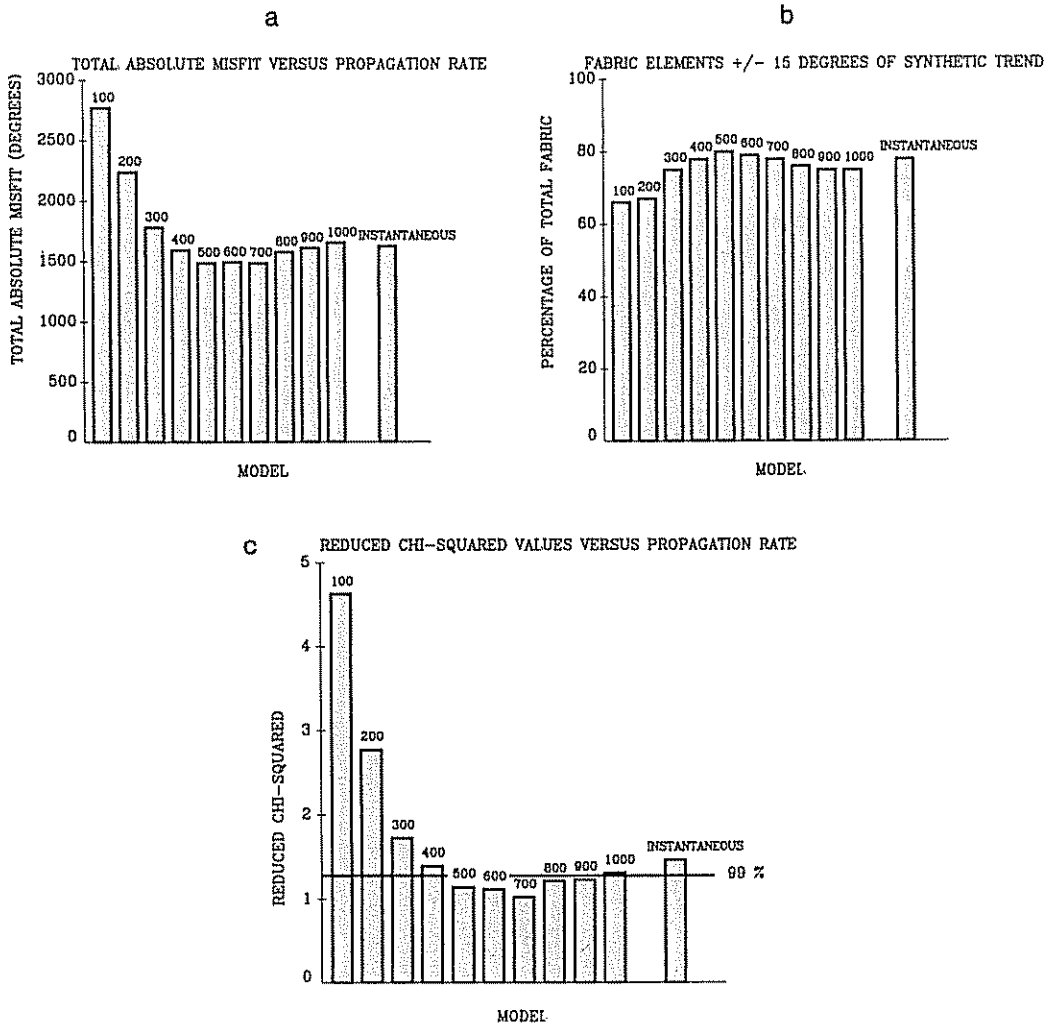

Fig. 7. Statistical analysis of the synthetic isochron fit to the fabric trends. (a) Total absolute value of misfit of the synthetic isochrons to the fabric. (b) Percent of synthetic isochrons parallel to within 15° of the fabric elements. (c) Reduced χ^2 values for this fit. The solid line represents the 99% confidence limit.

effect, however, does not have serious consequences for propagation rate assessment.

Although the 100 mm/yr model is clearly a poorer fit, the differences between the 500 and 1000 mm/yr models are more difficult to see because the predicted fabric changes orientation by only a few degrees. For example, the predicted trends in the Brunhes reoriented by event 5 change from 217° (100 mm/yr) to 196° (500 mm/yr) and finally to 191° (1000 mm/yr). The implication of multiple reorientations of fabric for estimating propagation rates is discussed in more detail below.

We attempted to quantify the misfits to different models using the difference between the 157 observed trends and the nearest predicted trend. The fit of different models is estimated in three ways (Fig. 7): (1) the number of fabric elements well fit (within 15° of observed trends) by the predicted fabric; (2) the total angular misfit to all the fabric data; and (3) a reduced χ^2 test. Figure 7a shows the total absolute misfit. Although the 500 mm/yr model fits best, the difference between this total misfit and the highest value in the 400–1000 mm/yr models is 171°, a little over 1° per fabric element. Figure 7b shows the percentage of fabric elements misfitting the nearest predicted trend by less than 15°. The 500 mm/yr model shows the best fit at 83%, but the difference between this value and the lowest value in the 400–1000 mm/yr models is only 6%. Figure 7c shows the reduced χ^2 values, assuming a standard deviation of 13° for the observed trends. This value was chosen in order to achieve a minimum reduced χ^2 value close to one. The standard deviation should ideally reflect the uncertainties associated both with interpretation and digitization of the imagery and measurement of trends. The minimum value occurs for a propagation rate of 700 mm/yr (Table 2), and the 99% confidence limits include propagation from 500 to 900 mm/yr.

It is unclear which test of misfit is the best. The percentage of elements fit is perhaps the most subjective; a 15° misfit is "good" whereas 16° is "bad". The total absolute misfit has the robustness associated with the median (L_1) norm, whereas the traditional χ^2 approach, while weighing outliers more heavily, allows for discrimination of the significance of model differences. Given that all three tests yield essentially the same result, and that this result seems consistent with the magnetics, any one is probably suitable, given the limitations of the data and modeling.

As is often the case with real data, it is difficult to assess what the true errors of measurements are and how well the error distribution approximates the Gaussian ideal. Systematic errors can also be present, e.g. fabric elements associated with seamounts were not digitized. Inclusion of the trends parallel to the most recent NSR trend does not seem to present a difficulty; the results are not significantly changed by deleting these data. Some

TABLE 2

Different criteria for the fit of the synthetic isochrons from the various models to the fabric

Model (mm/yr)	Percent of fabric ± 15°	Total degrees of misfit	Reduced χ^2
100	68	2833	4 62
200	69	2239	2 77
300	78	1781	1 72
400	81	1596	1 39
500	83	1486	1 14
600	82	1493	1 11
700	81	1487	1.02
800	80	1578	1.21
900	78	1612	1 23
1000	78	1657	1 31
Instantaneous	81	1626	1.46

The 95% reduced $-\chi^2$ confidence limit is 1.19 and that for the 99% confidence limit is 1.28

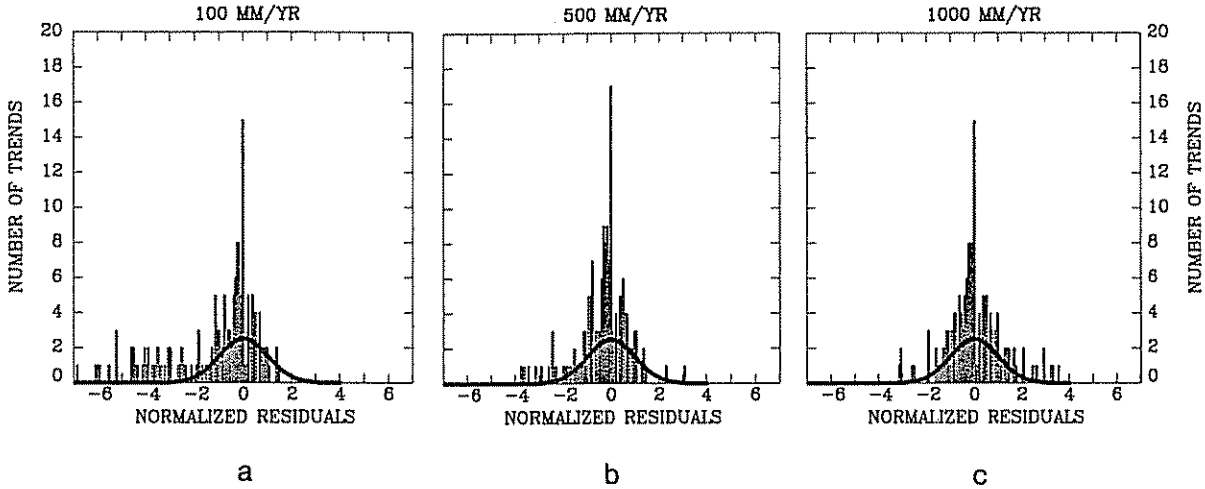

Fig. 8. Histograms of residual errors of the synthetic isochron fit to the fabric trends for the 100 mm/yr model (a), the 500 mm/yr model (b) and the 1000 mm/yr model (c). Note the shift in the asymmetric tails associated with each distribution. The synthetic trends systematically misfit the observations by a clockwise acute angle (negative residuals) in the 100 and, to a smaller extent, 500 mm/yr models. By 1000 mm/yr the acute angle of discrepancy is counter-clockwise (positive residuals), implying that we have swept through the best fit.

insight into the errors can be obtained from histograms of the normalized residuals (Fig. 8), which appear approximately Gaussian, with systematic misfits that give the asymmetric tails.

Discussion

These results suggest that, despite the obvious difficulties and limitations, numerical comparison of predicted and observed tectonic fabric trends can yield useful information on rift propagation kinematics. We feel that these results support Johnson et al.'s interpretation of the data as indicating propagation rates significantly in excess of spreading rates. This is gratifying given that their interpretation was based on magnetics alone, whereas Fig. 7 illustrates the effects of different propagation rates using only the fabric. We interpret our results as indicating that rates less than 300 mm/yr yield significantly poorer fits to the data, whereas rates faster than 900 mm/yr yield somewhat poorer fits.

These propagation rates are fast compared to many of those reported (Hey and Wilson, 1982; Hey et al., 1986; Caress et al., 1988; Naar and Hey, 1986; Macdonald et al., 1988; Mammerickx et al., 1988). Figure 9 shows some of the rift propagation and spreading rates reported at various sites along the East Pacific Rise. The squares represent rates averaged over a period of more than 2.0 Ma, typically by identifying pseudofaults

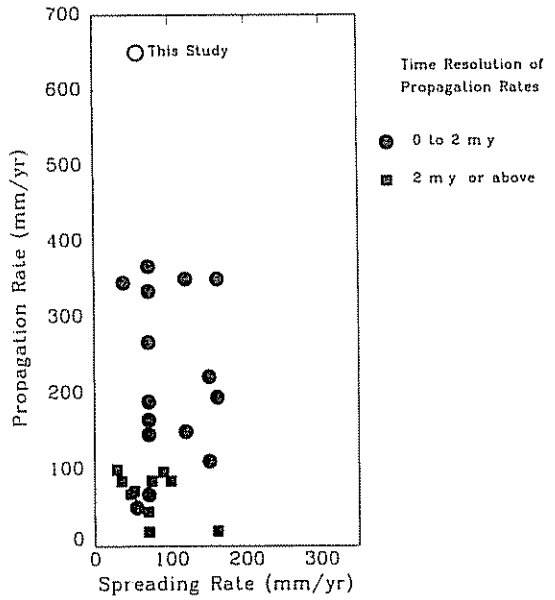

Fig. 9. Representative propagation rates versus averaged spreading rates from several propagating spreading centers reported along the East Pacific Rise. Squares denote rates determined from features which required 2 m.y. or more to form. Solid circles denote rates determined from features which required less than 2 m.y. to form. The open circle denotes the average rate for the Cobb from this study.

from the offset of seafloor magnetic lineations (Hey, 1977). The circles represent rates averaged over a period of less than 2.0 Ma, derived by identifying pseudofaults in the acoustic imagery (Macdonald et al., 1988), by offsets in rapid reversals of the magnetic isochrons (Caress et al., 1988) or by using seafloor fabric data (Macdonald et al., 1988; and this study). It is intriguing to note that studies using data which can resolve seafloor features on short timescales, tend to show episodes of fast propagation. This may result from propagation histories such as those inferred by Johnson et al. (1983) and Macdonald et al. (1988), in which individual propagation events occur quite rapidly, whereas the overall offsets evolve at slower rates.

Our modeling illustrates an interesting possible complication in estimating propagation rates for dueling propagator systems. This is due to the repeated reorientation of isochrons on lithosphere which has been transferred back and forth between plates during the propagation sequence. For a simple propagator geometry, in which the growing and dying rifts are parallel, the propagation rate can be found from the tangent of the angle between the reoriented isochrons and the rift trend, which equals the ratio of spreading rate to propagation rate (Searle and Hey, 1983; Acton et al., 1988). This is more complicated for dueling propagators, since material can be reoriented more than once.

Figure 10 shows a two-stage dueling propagator model, for which the first event is northward propagation at a rate equal to the spreading rate. Crust in the region labelled A has been reoriented such that the fabric trends 45° from its original position. A southward propagation event then occurs with a propagation rate equal to twice the spreading rate. This propagation event transfers crust in the region labelled B to the right-hand plate and reoriented the isochrons there by approximately 26.5°. In addition, the original reoriented material is split into two sections, A and A', such that the A' region is transferred back to the right-hand plate and isochrons there are reoriented even further. Propagation rates derived from the orientation of fabric in the unprimed regions would be correct, since the fabric has only been reoriented once. In contrast, the apparent propagation rate inferred from fabric in the primed region which has been reoriented twice, would equal 2/3 of the spreading rate, less than either of the actual propagation rates. Similarly, because a portion of a pre-existing pseudofault has been reoriented, an apparent propagation rate derived from it would not only be incorrect (equal to 1/2 the spreading rate), but different from the apparent propagation rate inferred from the multiple reoriented fabric. A slightly more complicated model is presented in Fig. 11. Here we consider a model with three events, each of which propagated at a rate equal to the spreading rate. As before, crust is transferred back and forth between the two plates within the overlap zone. Again, crust which has been transferred twice (regions A' and

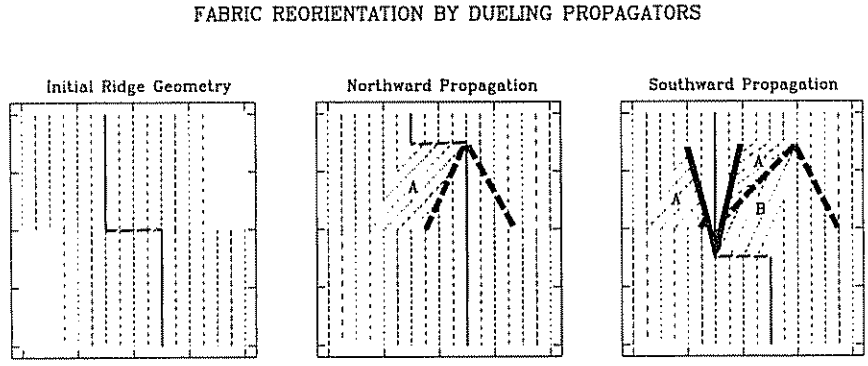

Fig. 10. Predicted fabric from a dueling model with two stages. Each stage propagates at a different rate, with the second stage propagating to the south twice as fast as the first stage propagated to the north. Isochrons in region A' have been transferred twice between plates, and hence reoriented twice. An apparent propagation rate inferred from the orientation of these lineations would be less than the true propagation rates. Heavy lines denote pseudofaults, and diagonally dashed lines represent active transform faults.

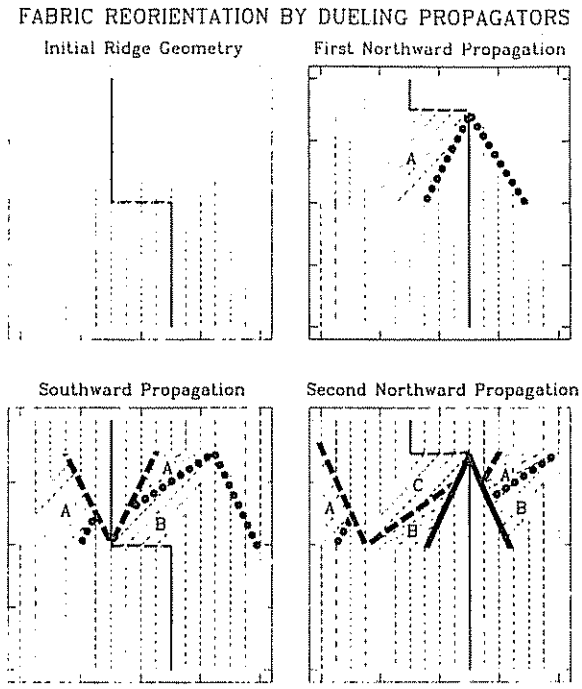

Fig. 11. Predicted fabric from a dueling propagator model with three stages, all of which propagate at the same rate. Isochrons in regions A' and B' have been transferred twice between plates, and hence reoriented twice. An apparent propagation rate inferred from the orientation of these lineations would be less than the true propagation rates. Heavy lines denote pseudofaults, and diagonally dashed lines represent active transform faults.

B') underwent two reorientations, so its orientation would imply spuriously slow propagation rates. For this example, the fabric reoriented twice would imply a 1:2 ratio between the apparent propagation rate and spreading rate. Similarly, a subsequent propagation event at the same rate could reorient fabric three times and imply a 1:3 ratio, and so on. Reoriented pseudofault trends predict propagation rates which are 2/3 of the spreading rate. Given these complexities, careful analysis may be required to correctly estimate propagation rates for dueling propagators.

We believe that the numerical modeling and comparison approach used here for the Cobb will be increasingly useful as additional lineation data for propagators become available. In the case of the Cobb Offset, in addition to indicating rapid propagation rates, the modeling has the interesting implication that the complex tectonic fabric does reasonably well fit on this scale (~1 km) by simple rift propagation models which do not invoke shear zone behavior and thus deviation from rigid plate tectonics. These techniques may thus be useful both in studying rift propagation parameters and in testing the level of model complexity required to fit a given set of data.

Acknowledgements

We thank Gary Acton and John Werner for technical assistance and Gary Acton, Richard Carlson, Donna Jurdy, Clyde Nishimura, and Mark Woods for their reviews of the manuscript. This research was supported by NSF grant EAR 8618038. Acknowledgement is also made to the donors of the Petroleum Research Fund, administered by the American Chemical Society, for partial support of this research.

References

Acton, G., Stein, S. and Engeln, J., 1988. Formation of curved seafloor fabric by changes in rift propagation velocity and spreading rate: application to the 95.5°W Galapagos propagator. J. Geophys. Res., 93: 11845–11861.

Acton, G., Stein, S. and Engeln, J., 1990. Block rotation and continental extension: a microplate model for Afar. Tectonics, 10: 501–526.

Anderson-Fontana, S., Engeln, J.F., Lundgren, P., Larson, R.L. and Stein, S., 1986. Tectonics and evolution of the Juan Fernandez microplate at the Pacific–Nazca–Antarctic triple junction. J. Geophys. Res., 91: 2005–2018.

Atwater, T., 1989. Plate tectonic history of the Northeast Pacific and Western North America. In: E.L. Winterer, D.M. Hussong and R.W. Decker (Editors), The Eastern Pacific Ocean and Hawaii, The Geology of North America, N. Geological Society of America, Boulder, Colo., pp. 21–72.

Caress, D.W., Menard, H.W. and Hey, R.N., 1988. Eocene reorganization of the Pacific–Farallon spreading center north of the Mendocino fracture zone. J. Geophys. Res., 93: 2813–2838.

Carlson, R.L., 1981. Late Cenozoic rotations of the Juan de Fuca Ridge and the Gorda Rise: a case study. Tectonophysics, 77: 171–188.

Courtillot, V., Galdeano, A. and Le Mouel, J.L., 1980. Propagation of an accreting plate boundary: a discussion of new aeromagnetic data in the Gulf of Tadjurah and southern Afar. Earth Planet. Sci. Lett., 47: 144–160.

Davis, E., Currie, R. and Sawyer, B., 1987. Acoustic imagery: North Central Juan de Fuca Ridge. Map 16–1987, Geological Society of Canada, Ottawa, Ont.

Engeln, J F and Stein, S, 1984 Tectonics of the Easter plate Earth Planet Sci Lett, 68: 259–270

Engeln, J F, Stein, S, Werner, J and Gordon, R, 1988 Microplate and shear zone models for oceanic spreading center reorganizations, J Geophys Res, 93: 2839–2856

Francheteau, J, Yelles-Chaouche, A and Craig, H, 1987 The Juan Fernandez microplate near the Pacific–Nazca–Antarctic plate junction at 35°S Earth Planet Sci Lett, 86: 253–268

Hey, R, 1977 A new class of "pseudofaults" and their bearing on plate tectonics: A propagating rift model Earth Planet Sci Lett, 37: 321–325

Hey, R and Vogt, P, 1977 Spreading center jumps and sub-axial asthenosphere flow near the Galapagos hotspot Tectonophysics, 37: 41–52

Hey, R N and Wilson, D S, 1982 Propagating rift explanation for the tectonic evolution of the Northeast Pacific—the pseudomovie Earth Planet Sci Lett, 58: 167–188

Hey, R, Duennebier, F K and Morgan, W J, 1980 Propagating rifts on mid-ocean ridges J Geophys Res, 85: 3647–3658

Hey, R N, Naar, D F, Kleinrock, M C, Morgan, W J P, Morales, E and Schilling, J-G, 1985 Microplate tectonics along a superfast seafloor spreading system near Easter Island Nature, 317: 320–325

Hey, R N, Kleinrock, M C, Miller, S P, Atwater, T M and Searle, R C, 1986 Sea Beam/Deep-Tow investigation of an active oceanic propagating rift system, Galapagos 95 5°W J Geophys Res, 91: 3369–3393

Johnson, H P, Karsten, J L, Delaney, J R, Davis, E E, Currie, R G and Chase, R L, 1983 A detailed study of the Cobb offset of the Juan de Fuca Ridge: evolution of a propagating rift J Geophys Res, 88: 2297–2315

Karsten, J L, Hammond, S R, Davis, E E and Currie, R G, 1986 Detailed geomorphology and neotectonics of the Endeavour Segment, Juan de Fuca Ridge: new results from Seabeam swath mapping Geol Soc Am Bull, 97: 213–221

Lonsdale, P, 1989 The rise flank trails left by migrating offsets of the Equatorial East Pacific Rise axis J Geophys Res, 94: 713–743

Macdonald, K C, Haymon, R M, Miller, S P, Sempere, J-C and Fox, P J, 1988 Deep-Tow and Sea Beam studies of dueling propagating ridges on the East Pacific Rise near 20°40'S J Geophys Res, 93: 2875–2898

Mammerickx, J, 1984 The morphology of propagating spreading centers: new and old J Geophys Res, 89: 1817–1828

Mammerickx, J, Naar, J F and Tyce, R L, 1988 The Mathematician paleoplate J Geophys Res, 93: 3025–3040

McKenzie, D P, 1986 The geometry of propagating rifts Earth Planet Sci Lett, 77: 176–186

Miller, S P and Hey, R N, 1986 Three-dimensional magnetic modeling of a propagating rift, Galapagos 95°30'W J Geophys Res, 91: 3395–3406

Naar, D F and Hey, R N, 1986 Fast rift propagation along the East Pacific Rise near Easter Island J Geophys Res, 91: 3425–3438

Nishimura, C, Wilson, D S and Hey, R N, 1984 Pole of rotation analysis of present-day Juan de Fuca plate motion J Geophys Res, 89: 10283–10290

Raff, A D and Mason, R G, 1961 Magnetic survey off the west coast of North America, 40°N latitude to 50°N latitude Geol Soc Am Bull, 72: 1267–1270

Riddihough, R P, 1977 A model for recent plate interactions off Canada's west coast Can J Earth Sci, 14: 384–396

Riddihough, R P, 1984 Recent movements of the Juan de Fuca plate system J Geophys Res, 89: 6980–6994

Searle, R C and Hey, R N, 1983 Gloria observations of the propagating rift at 95 5°W on the Cocos–Nazca spreading center J Geophys Res, 88: 6433–6448

Stoddard, P R, 1987 A kinematic model for the evolution of the Gorda plate J Geophys Res, 92: 11524–11532

Vine, F J, 1966 Spreading of the ocean floor: new evidence Science, 154: 1405–1415

Vine, F J and Wilson, J T, 1965 Magnetic anomalies over a young ocean ridge off Vancouver Island Science 150: 485–489

Vink, G E, 1982 Continental rifting and the implications for plate tectonic reconstructions J Geophys Res, 87: 10677–10688

Wilson, D S, 1988 Tectonic history of the Juan de Fuca Ridge over the last 40 million years J Geophys Res, 93: 11863–11876

Wilson, D S, Hey, R N and Nishimura, C, 1984 Propagation as a mechanism of reorientation of the Juan de Fuca Ridge J Geophys Res, 89: 9215–9225